Nanostructured copper selenide as an ultrasensitive and selective non - enzymatic glucose sensor

Received 00th January 20xx,
Accepted 00th January 20xx

DOI: 10.1039/x0xx00000x

Siddesh Umapathi,[a] Harish Singh,[a] Jahangir Masud[b] and Manashi Nath[a]*

CuSe nanostructures exhibit high-efficiency for glucose detection with high sensitivity (19.419 mA mM^{-1} cm^{-2}) and selectivity at low applied potential of +0.15 V vs Ag|AgCl, low detection limit of 0.196 µM and linear range of glucose detection from 100 nM - 40 µM.

Diabetes caused by the imbalance of glucose level in blood has been of severe concern lately, leading to 1.5 million deaths across the globe according to World Health organization reports. It has also been predicted that diabetes will become 7th leading cause of mortality by 2030.[1-4] Diabetes is a silent killer where the symptoms may not be expressed until a very advanced stage leading to more fatality. Hence, continuous monitoring of blood glucose levels in susceptible as well as healthy individuals is very important to detect onset of diabetes at an early stage and minimize progression of the disease by taking preventive measures. While commercially available enzyme-based glucose sensing strips are widely used for measuring blood glucose levels, their limited shelf life, low sensitivity, non-reusability, and high cost, makes it desirable to seek alternate solutions for glucose sensing. [5-7] Moreover, non-enzymatic glucose sensors are also lucrative for long-term continuous blood glucose monitoring systems that can be implanted in peripheral tissue including sub-dermis or tooth enamel. Electrochemical glucose sensors work on the principle of direct glucose oxidation on the electrocatalytic surface, and can be categorized into two types: the enzymatic and non-enzymatic glucose sensors.[8-10] Among these the non-enzymatic glucose sensors have attracted considerable attention over the last few years attributed to their advantages such as high stability and sensitivity, low cost, and simple preparation.[11-13]

Over the last several years various non-enzymatic glucose sensors based on different kinds of materials have been reported, such as metal nanoparticles and carbon materials, where polymer binders have been used to immobilize these nanoparticles. Such non-conductive polymeric binders add inactive component in the catalytic composite which may hinder the ability for quick electron transfer within the catalytic composite and reduce sensitivity.[14-17] On the other hand, transition metals consisting of Ni, Co and Fe have been demonstrated as promising materials towards glucose oxidation which also have the advantage of being earth abundant, low cost and environmental friendly.[18-22] Multi metal alloy and multi metallic compounds such as Co-Ni, Ni-Fe and Ni-Cu have also shown good electrochemical glucose sensing.[23-26]

In recent years, transition metal chalcogenides has gained considerable attention in electrochemical devices such as water electrolyzer, fuel cells, and as supercapacitors, owing to their unprecedented high electrocatalytic activity. This improvement of electrochemical activity of TMC is primarily caused by reduced anion electronegativity and high degree of covalency in the lattice which leads to better electrochemical tunability and reduced bandgap in the materials. While the electrochemical tunability aids in adsorption of reactive intermediates on the catalyst surface through local oxidation/reduction of the transition metal active site, a reduced bandgap also enhances the charge transport at the catalyst-electrolyte interface as well as through the catalyst composite.[27-29] The effect of decreasing anion electronegativity on the electrocatalytic activity has been recently observed in a series of Ni-chalcogenide water oxidation catalysts where it was observed that the catalytic efficiency progressively improves from Ni-oxide to Ni-telluride.[30-32] Copper has been studied recently for its electrochemical activity in various systems, and presents as attractive case for further expansion attributed to its abundancy on earth's surface, and low-cost.[33-35] These attributes has led to the usage of Cu in various catalytic processes.[36] However, reports of copper chalcogenides in electrochemical devices are still limited. As explained above, decreasing anion electronegativity is expected to improve the electrochemical tunability of the catalytically active transition metal center leading to better electrocatalytic activity.

In this communication, we have reported a high efficiency, non-enzymatic, direct glucose electrochemical sensor based on CuSe nanostructures synthesized by one step electrodeposition directly on the electrode surface as well as by hydrothermal techniques. Such direct growth on the electrode surface avoids the use of any adhesive or polymeric binder which can reduce sensing performance. The as-prepared CuSe shows excellent sensitivity and low limit of detection for detection of glucose. The developed sensor was also applied successfully for the detection of glucose in human blood samples.

D-Glucose, copper chloride, selenium oxide and NaOH were purchased from Arcos chemicals. Uric acid (UA), l-ascorbic acid (AA), dopamine (DA), NaCl and KCl were obtained from Alfa Aesar. All chemicals were used as received without any further purification. Deionized water was used in all experiments.

[a] *Department of Chemistry, Missouri University of Science and Technology, Rolla, USA*
[b] *Energy and Environmental Research centre, University of North Dakota, Grand Forks, USA*

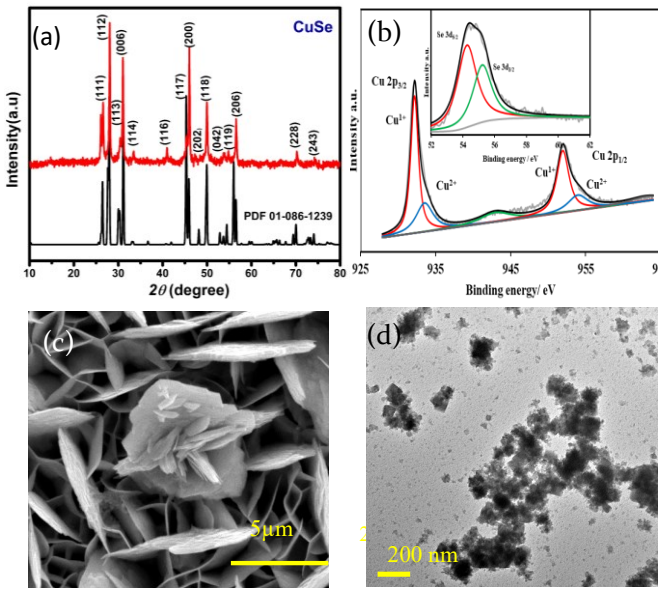

Fig. 1. (A) PXRD pattern of hydrothermally synthesized CuSe, compared with reference pattern (PDF#00-086-1239) (* denotes Au peaks). (B) Deconvoluted XPS spectra of CuSe showing Cu 2p peaks. Inset in (b) shows the corresponding Se 3d signals. (C) SEM and (D) TEM images of CuSe.

The CuSe thin film was prepared directly on a carbon cloth electrode through direct electrodeposition using a conventional three electrode set-up, where Ag|AgCl was used as the reference electrode, graphite rod as the counter electrode and commercial carbon cloth as the working electrode. The deposition area of CuSe was pre-defined by using a masking tape exposing a 0.08 cm^2 hole on the electrode surface. The electrolyte contained 2 mM of copper chloride, 4.5 mM SeO_2 and 0.1 M of KCl in deionized water. The pH of the electrolyte was adjusted to 2 using dilute HCl. This solution was purged with N_2 gas for 20 minutes prior to electrodeposition to reduce amount of dissolved air. Electrodeposition was carried out at an applied voltage of -0.16 V vs Ag|AgCl for 300 seconds. Following electrodeposition, the substrate was mildly washed with DI water and dried naturally. CuSe powder was also synthesized through hydrothermal techniques as described in the supporting information.

The composition, phase, and morphology of the copper selenide catalyst composite was identified through powder X-ray diffraction (pxrd), scanning electron microscopy (SEM) (FEI Helios Nanolab 600) using 10kV accelerated voltage, and Energy dispersive spectroscopy (EDS). Composition of the film was also analyzed through X-ray photoelectron spectroscopy (XPS) using KRATOS AXIS 165 spectrometer with Al source. Transmission electron microscopy (Tecnai F20 with an accelerating voltage of 200 kV) was also performed to investigate nanostructure details of the morphology. Electrochemical measurements were performed using Iviumstat electrochemical workstation using a three-electrode system with CuSe on carbon cloth as working electrode, saturated Ag|AgCl as reference electrode and a graphite rod served as counter electrode.

The pxrd pattern collected from hydrothermally synthesized copper selenide powder, showed highly crystalline pattern as shown in Fig. 1A confirming phase purity and composition of the catalyst. The diffraction pattern matched with the standard diffraction pattern for CuSe (PDF# 00-086-1239) confirming the phase. CuSe crystallizes in a hexagonal structure with Cu in two different coordination geometries, trigonal planar and tetrahedral. Such low coordination geometries around the active sites are expected to enhance adsorption of oxygenated reactive intermediates on the surface through coordination expansion leading to improved electrocatalytic performance as has been observed previously in other transition metal selenide based electrocatalyst.[32] . The composition of the as-deposited film was confirmed through XPS, which also provides details of local bonding environment and oxidation states of the elements. As shown in Fig. 1B the Cu 2p spectrum shows peaks centered at 932.2 and 952.3 eV for Cu^+ $2p_{3/2}$ and $2p_{1/2}$ and 934.4 and 954.6 eV for Cu^{2+} $2p_{3/2}$ and $2p_{1/2}$ respectively. This also suggested that Cu was present in mixed oxidation states, while the satellite peaks are observed at 942.4 and 962.6 eV. The deconvoluted Se 3d spectra of electrodeposited CuSe (inset of Fig. 1B) shows peaks at 54.4 and 55.4 eV for Se $3d_{5/2}$ and $3d_{3/2}$ respectively which is in accordance to previously reported copper selenide.[37]

The SEM images of as-deposited CuSe thin film as depicted in Fig. 1C showed that CuSe had a rough surface topology comprising nanoflake like morphology. The nanoflakes are randomly oriented leading to a porous film which provides high surface area for the glucose adsorption. The elemental mapping through EDS showed uniform distribution of Cu and Se throughout the composite, while quantification of the EDS data yielded an elemental ratio of 1: 1 for Cu: Se (Fig. S1). TEM studies (Fig. 1D) showed similar flake-like nanostructures while HRTEM images showed the lattice fringes corresponding to a d- spacing of 3.31 Å which could be matched to 101 lattice spacing of CuSe (Fig. S2).

The electrocatalytic performance of CuSe thin film towards oxidation of glucose was studied by cyclic voltammogram (CV). Fig. 2A shows the CV of CuSe thin film on carbon cloth measured in presence and absence of 0.1 mM glucose in 0.1 M NaOH electrolyte at 10 mV/s scan rate. While the current response was moderate in a blank 0.1 M NaOH electrolyte, upon addition of 0.1 mM of glucose into the alkaline electrolyte, there was a substantial increase in the anodic current, indicating oxidation of glucose on the CuSe-coated electrode. This oxidation was also observed in the reverse sweep of CV, which further confirmed the process to be analyte, i.e. glucose oxidation on the electrode surface. To further evaluate the electrocatalytic performance of CuSe towards glucose oxidation, the scan rates were varied from 5 mV/s to 75 mV/s as shown in Fig. 2B. The glucose oxidation peaks shows obvious trend in the increase of current with respect to the scan rate in addition to a positive shift of the anodic potential. The redox peak current showed a linear correlation (R^2 = 0.9965) with square root of the scan rate, which is typical for a diffusion-controlled process for any electrochemical oxidation. On addition of 0.25, 0.5, 1, 2 and 4 mM of glucose to 0.1 M NaOH solution, CuSe composite electrode showed an increase in the current density corresponding to the increase in glucose concentration (Fig. 2C), indicating that the oxidation current is mainly due to the availability of increased glucose content in the electrolyte.

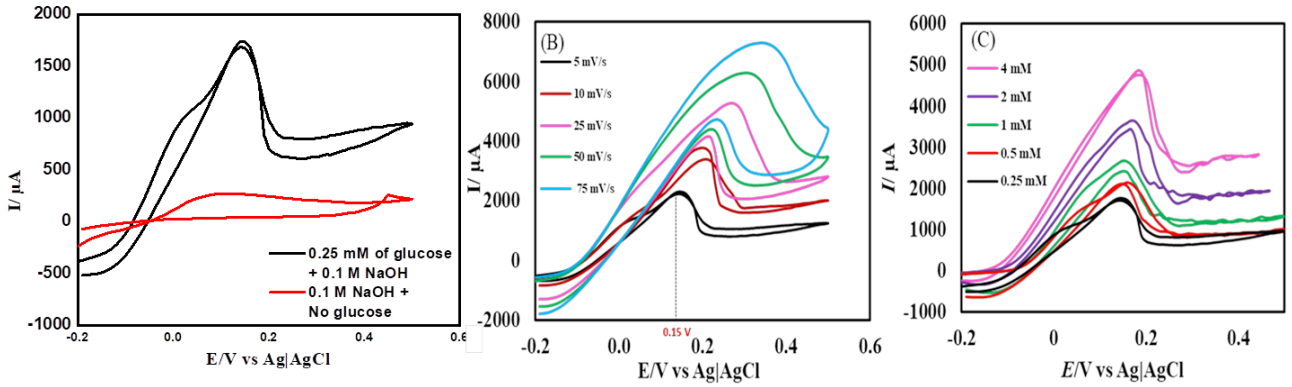

Fig. 2. (A) CV curves of CuSe with 0.25 mM glucose and no glucose in 0.1 M NaOH solution. (B) CV plots with scan rates ranging from 5 to 75 mV/s. (C) CV curves of CuSe with varying concentrations of glucose ranging from 0.25 mM to 4 mM.

In order to determine the optimal applied potential for glucose sensing, the oxidation current was measured by scanning the potential ranging from 0.05 V to 0.3 V vs Ag|AgCl using amperometric technique with successive addition of 0.1 mM glucose to the 0.1 M NaOH electrolyte under constant stirring. Fig. S3 shows that the ratio of oxidation current vs the potential range from 0.05 V to 0.30 V, where the highest oxidation current was achieved at 0.15 V, after which it begins to decay. Hence, the ideal working potential for oxidation of glucose at electrodeposited CuSe thin film was selected to be +0.15 V vs Ag|AgCl for the rest of the study.

Similar electrochemical measurements were also performed for the hydrothermally synthesized CuSe powder assembled on the electrode as described in supporting information. The hydrothermally synthesized CuSe powder showed enhanced glucose oxidation at 0.25 V vs Ag|AgCl as shown in Fig. S4.

Chronoamperometric technique was used to measure the response of CuSe composite electrode upon successive injections of glucose in a homogenously stirred NaOH solution. As a control experiment, current response upon successive addition of glucose was also measured from a bare carbon cloth electrode to confirm that the current increments observed are not due to accidental jumps due to experimental conditions. The limit of detection and linear range were also determined using the above method. As shown in Fig. 3A, a constant potential of +0.15 V vs Ag|AgCl was applied, when CuSe-modified electrodes showed a rapid and significant response of increasing anodic current upon addition of glucose ranging from 100 nM to 5 mM, which indicates the high sensitivity of CuSe towards glucose sensing. The bare carbon electrode on the other hand, did not show any response on successive addition of glucose as shown in Fig. S5(a) in supporting information. Additional control experiments were also performed by adding 100 µL of PBS (0.1 M) and 100 µL of DI water separately to the

Table 1. Comparison of Performance of Various Copper Based Nonenzymatic Glucose Sensors

Electrode	Applied potential (/V vs Ag|AgCl)	Sensitivity (mA mM^{-1} cm^{-2})	Linear range	LOD (µM)	Ref
CuSe (electrodeposition)	0.15	19.41	100 nM-80µM; 100µM-5mM	0.196	This work
CuSe (hydrothermal)	0.25	8.314	10 – 80 µM; 320 µM – 2 mM	0.391	This work
CuO nanowires	0.55	0.648	-	2	[12]
Cu2Se SPs/CF	0.50	18.66	0. 25 µM –0.237 mM	0.25	[35]
CuO NWA/CF	0.50	32.33	0.10 mM–0.50 mM	0.02	[41]
CuNi/C Nanosheet	0.54	17.12	0.2 µM –2.72 mM	0.066	[42]
Cu@porous carbon	0.55	10.1	1µM–6.0 mM	0.6	[43]
CuS/RGO/CuS/Cu	0.65	22.67	0.001–0.655 mM	0.5	[44]
CuO NPs	0.50	1.430	0.04–6.0 mM	5	[45]
CuCo2O4 NWAs/CC	0.55	3.930	0.001–0.93 mM	0.5	[46]
CuO/rGO/CNT	0.60	9.278	0.01–1 mM	1	[47]
CuO/NiO/PANI/GCE	0.60	3.402	20 µM –2.5 mM	2	[48]
CuO–ZnO NRs/FTO	0.62	2.961	Up to 8.45 mM	0.4	[49]

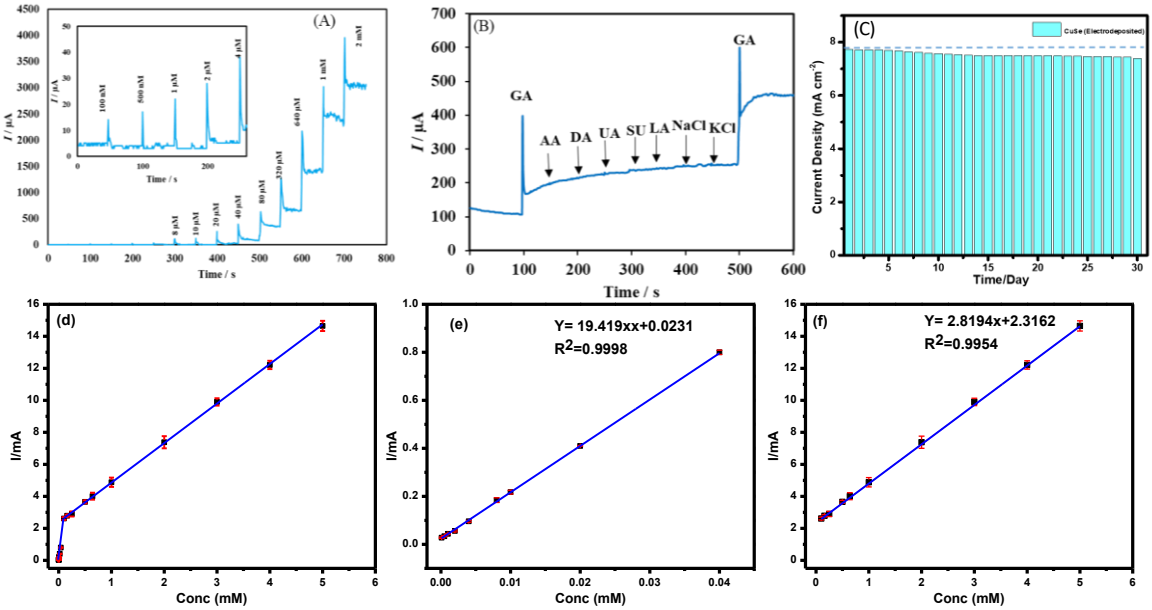

Fig. 3. (A) Chronoamperometric response of the CuSe-modified electrode to successive additions of glucose into stirred 0.1M NaOH electrolyte. The working potential was set at +0.15 V vs Ag|AgCl, and the glucose concentrations ranged from 100 nM to 2 mM for sequential addition. Inset shows magnified portion of the amperometric response for lower concentrations of glucose addition. (B) Amperometric response of CuSe-modified electrode measured in 0.1M NaOH with successive addition of glucose (0.1 mM), AA (0.5 mM), DA (0.5 mM), UA (0.5 mM), Sucrose (0.1 mM), Lactose (0.1 mM), NaCl (0.5 mM), KCl (0.5 mM), and glucose (0.1 mM) at an applied potential of +0.15 V vs Ag|AgCl. (c) Long-term stability check for 30 days of CuSe electrodes by addition of 1mM glucose solution each day for over 30 days. (d) Peak current versus the concentration of glucose at low and high concentration regions for electrodeposited CuSe. (e) Linear range from 100 nM to 40 µM and (f) linear range from 100 µM to 5 mM.

electrolyte for checking the instantaneous current response in absence of glucose. As shown in Fig. S5(b), there was no instantaneous current response upon addition of PBS or DI water in the same electrolyte, indicating that the current response upon addition of glucose solution is the actual sensing current. The calibration curve was obtained by plotting the peak anodic current vs concentration of glucose from the amperometric experiment described above. Fig. 3(d-f) shows the calibration curve from 100 nM to 5 mM where the corresponding regression equation can be described as I (mA) = 19.419C (mM) + 0.0231 (R2 = 0.9998) having a high sensitivity of 19.419 mA mM^{-1} cm^{-2}. Further the linear detection range of CuSe towards glucose was 100 nM to 40 µM and a second linear region for higher concentrations from 80 µM to 5 mM, with a limit of detection of 196 nM. Fig. S6 shows the response time of CuSe upon addition of glucose. The catalyst achieves steady state current within 2 sec of glucose addition, which shows that these CuSe-modified electrodes is capable of real time monitoring of glucose in the body. Chronoamperometric measurements were also performed with hydrothermally synthesized CuSe powder as shown in Fig. S7a, which showed a sensitivity of 8.341, and first and second linear detection range of 10 µM -80 µM and 320 µM-2 mM of glucose detection respectively (Fig. S8(a-c)). A slightly lower sensitivity for the hydrothermally synthesized powder can be attributed to the fact that the electrode contains Nafion which restricts exposure of the catalytic site to glucose in the electrolyte. Nevertheless, the CuSe-based electrodes shows high sensitivity for glucose detection with low LOD compared to other non-enzymatic glucose sensors as shown in Table 1.

Several biomolecules with similar oxidation profiles are known to interfere in detection of glucose which makes the development of nonenzymatic glucose sensors very challenging. Species such as ascorbic acid (AA), dopamine (DA), lactose, NaCl and KCl commonly available in lower concentration in bodily fluids can exhibit interference by undergoing electro-oxidation. Therefore, the selectivity of CuSe towards glucose oxidation was confirmed by measuring amperometric response of CuSe composite electrode upon consecutive injection of glucose and other interferents as mentioned above. A constant potential of +0.15 v vs Ag|AgCl was applied to an evenly stirred 0.1 M NaOH solution wherein, addition of 0.1 mM of glucose showed rapid increase of anodic current. Addition of sucrose and lactose (0.1 mM) and AA, DA, LC, NaCl, KCl (0.5 mM) did not show any appreciable oxidation current. However, the second addition of 0.1 mM glucose showed similar jump in anodic current density as observed from the 1st addition which validated the functionality and selectivity of the CuSe based composite electrode was (Fig. 3B). Interference studies were also conducted with hydrothermally synthesized CuSe powder which shows similar selectivity for glucose oxidation at low applied potential as shown in Fig. S7b (supporting information). Thus, it was confirmed that CuSe exhibits high sensitivity and selectivity for non-enzymatic glucose sensing at an extremely low working potential.

To confirm long-term functional stability of CuSe electrodes, glucose oxidation currents were measured by exposing the same CuSe-coated electrode repeatedly to 1mM glucose solution each day for over 30 days. The electrode being used was stored under ambient conditions. It was observed that even after being exposed to air for 30 days, both electrodeposited and hydrothermally synthesized CuSe-modified electrodes retained more that 90% of their original current response as shown in Fig. 3C and S7c for electrodeposited and hydrothermally synthesized CuSe, respectively. Such studies confirmed the long-term stability of these electrodes.

The practical applicability of the fabricated non-enzymatic glucose sensor was investigated by the determination of glucose in human blood samples using a known method[38] and comparing it with the commercially available enzymatic glucometer kit (ReliOn). Specifically, the experiment comprised of first stabilizing current response of the electrode by adding 1mM of glucose two times. The blood sample was then injected directly to the NaOH electrolyte in the vicinity of the CuSe-modified electrode. 1mM of glucose was added again and the current response was recorded. The glucose level in the blood samples was measured from linear fit of the plot obtained by plotting the current density vs glucose concentration of standard glucose additions as shown in Fig. S9. The range of chronoamperometry measurements were also extended to much higher glucose concentration, specifically, 0.1 mM to 5 mM in Order to match human blood glucose concentration (Fig S10). Table 2 lists the glucose concentration as detected by a standard glucometer and the CuSe based sensor. Each sample was tested three times and the calculated relative standard deviation of less than 3% suggests the robustness and reliability of CuSe towards glucose sensing in physiological samples.

Table 2. Results of Glucose Detection in Human Blood

Sample	Glucometer (mM)	CuSe (mM)	RSD (%, n=3)
1st glucose	6.37	6.39	1.4
2nd glucose	4.72	4.84	3.59
3d glucose	5.7	5.55	2.4
Blood 1	5.45	5.56	2.6
Blood 2	5.48	5.5	2.1
Blood 3	5.18	5.25	2.5
Blood 4	4.66	4.75	2.4

Owing to its high sensitivity, short response time and low detection limit electrodeposited CuSe is a potential candidate for continuous glucose monitoring system for commercial applications. Additionally, CuSe has a low working potential and selectivity to sense glucose and not the other biomolecules commonly present in bodily fluids which is an advantage to use in wearable biosensors. Other than biosensing, CuSe has also been reported for electrochemical energy conversion.[39] The superior electrochemical performance of CuSe especially towards glucose oxidation can be attributed to several factors. The initial step of glucose oxidation is the activation of the catalyst achieved by attachment of the molecule on the electrode surface through the coordination of the -OH functional group on the catalytically active transition metal site (Cu). Such -OH attachment proceeds through local site oxidation of the active site. Previously we have shown the -OH adsorption can be facilitated by controlling the ligand environment, typically by decreasing anion electronegativity,[31] which reduces the required potential for catalyst activation, thereby increasing efficiency.[40] Moreover, Cu in copper selenide has mixed oxidation states. In case of Cu^{+} and Se^{2-} we can expect a certain degree of polarization due to charge imbalance. However, in case of Cu^{2+} there is increase in the covalency between Cu-Se bonds. This mixed oxidation states leads to inductive effect and redistribution of electron density at metal sites through *d-d* interactions, which is favorable for –OH groups to adsorb. Additionally, replacing oxides with less electronegative selenides also leads to increased covalency in the lattice and enhances the redox activity at Cu site which consequently has an effect on the reversible electrochemical response. The low potential required for glucose oxidation is advantageous for making affordable and energy efficient non-enzymatic glucose sensors.

In conclusion simple, binary copper selenide has been identified as a highly efficient, non-enzymatic, electrochemical glucose biosensor with low limit of detection and high sensitivity. The CuSe was synthesized directly on the electrodes by electrodeposition producing a porous morphology comprising flake-like nanostructures. The electrocatalytic activity for glucose oxidation was studied in alkaline conditions. Electrodeposited CuSe exhibited superior efficiency for glucose oxidation with a sensitivity of 19.419 mA mM^{-1} cm^{-2} and a low detection limit of 0.196 µM, has a wide linear range 100 nM - 40 µM and fast response time of less than 2 s, long term stability and excellent selectivity. These attributes ensure that this system will be able to reliably detect very small fluctuation in glucose level in even bodily fluids such as urine, sweat, tears, tissue fluids etc., which has very low concentration of glucose. Additionally, the glucose oxidation at CuSe-modified electrodes occurs at very low working potential of +0.15 V vs Ag|AgCl which increases the energy efficiency of the system. These results reveal a great potential of electrodeposited CuSe as a high-efficiency glucose sensor with practical applicability.

Acknowledgement

This work was partially supported by NSF DMR-1710313.

Conflicts of interest

The authors declared they have no conflict of interest to this work.

Corresponding Author

* E-mail: nathm@mst.edu

Notes and references

Supporting information available: SEM and HRTEM images, i-V plots and i-t plot.

1 K. M. Bullard, C. C. Cowie, S. E. Lessem, S. H. Saydah, A. Menke, L. S. Geiss, T. J. Orchard, D. B. Rolka and G.

Imperatore, *MMWR Morb Mortal Wkly Rep*, 2018, **67**, 359-361.
2 A. L. Galant, R. C. Kaufman and J. D. Wilson, *Food Chemistry*, 2015, **188**, 149-160.
3 A. T. Kharroubi and H. M. Darwish, *World J Diabetes*, 2015, **6**, 850-867.
4 A. Stokes and S. H. Preston, *PLoS One*, 2017, **12**, e0170219-e0170219.
5 G. Rocchitta, A. Spanu, S. Babudieri, G. Latte, G. Madeddu, G. Galleri, S. Nuvoli, P. Bagella, M. I. Demartis, V. Fiore, R. Manetti and P. A. Serra, *Sensors*, 2016, **16**, 780.
6 R. Gaia, S. Angela, B. Sergio, L. Gavinella, M. Giordano, G. Grazia, N. Susanna, B. Paola, D. Maria Ilaria, F. Vito, M. Roberto and S. Pier Andrea, *Sensors*, 2016, **16**, 780-780.
7 R. Wilson and A. P. F. Turner, *Biosen. Bioelectron.*, 1992, **7**, 165-185.
8 E.-H. Yoo and S.-Y. Lee, *Sensors (Basel)*, 2010, **10**, 4558-4576.
9 J. Wang, *Chem. Rev.*, 2008, **108**, 814-825.
10 A. Harper and M. R. Anderson, *Sensors*, 2010, **10**, 8248-8274.
11 P. Si, Y. Huang, T. Wang and J. Ma, *RSC Adv.*, 2013, **3**, 3487-3502.
12 Y. Zhang, Y. Liu, L. Su, Z. Zhang, D. Huo, C. Hou and Y. Lei, *Sens. Actuators, B*, 2014, **191**, 86-93.
13 Y. Mu, D. Jia, Y. He, Y. Miao and H.-L. Wu, *Biosens. Bioelectron.*, 2011, **26**, 2948-2952.
14 A. A. Saei, J. E. N. Dolatabadi, P. Najafi-Marandi, A. Abhari and M. de la Guardia, *TrAC, Trends Anal. Chem.*, 2013, **42**, 216-227.
15 J. Luo, S. Jiang, H. Zhang, J. Jiang and X. Liu, *Anal. Chim. Acta*, 2012, **709**, 47-53.
16 H.-X. Wu, W.-M. Cao, Y. Li, G. Liu, Y. Wen, H.-F. Yang and S.-P. Yang, *Electrochim. Acta*, 2010, **55**, 3734-3740.
17 Z. Zhu, L. Garcia-Gancedo, A. J. Flewitt, H. Xie, F. Moussy and W. I. Milne, *Sensors*, 2012, **12**, 5996-6022.
18 Y. Zhang, Y. Wang, J. Jia and J. Wang, *Sens. Actuators, B*, 2012, **171-172**, 580-587.
19 P. Vennila, D. J. Yoo, A. R. Kim and G. G. kumar, *J. Alloys Compd.*, 2017, **703**, 633-642.
20 T. Chen, D. Liu, W. Lu, K. Wang, G. Du, A. M. Asiri and X. Sun, *Anal. Chem.*, 2016, **88**, 7885-7889.
21 P. K. Kannan and C. S. Rout, *Chem. - Eur. J.*, 2015, **21**, 9355-9359.
22 X. Niu, M. Lan, H. Zhao and C. Chen, *Anal. Chem.*, 2013, **85**, 3561-3569.
23 K. Ramachandran, T. Raj kumar, K. J. Babu and G. Gnana kumar, *Sci. Rep.*, 2016, **6**, 36583.
24 J. Yang, X. Liang, L. Cui, H. Liu, J. Xie and W. Liu, *Biosens. Bioelectron.*, 2016, **80**, 171-174.
25 M. Ranjani, Y. Sathishkumar, Y. S. Lee, D. Jin Yoo, A. R. Kim and G. Gnana kumar, *RSC Adv.*, 2015, **5**, 57804-57814.
26 P. V. Suneesh, V. Sara Vargis, T. Ramachandran, B. G. Nair and T. G. Satheesh Babu, *Sens. Actuators, B*, 2015, **215**, 337-344.
27 A. T. Swesi, J. Masud, W. P. R. Liyanage, S. Umapathi, E. Bohannan, J. Medvedeva and M. Nath, *Sci. Rep.*, 2017, **7**, 2401-2401.
28 M. Pumera, Z. Sofer and A. Ambrosi, *J. Mater. Chem. A*, 2014, **2**, 8981-8987.
29 M.-R. Gao, J. Jiang and S.-H. Yu, *Small*, 2012, **8**, 13-27.
30 S. Umapathi, J. Masud, A. T. Swesi and M. Nath, *Adv. Sustainable Syst.*, 2017, **1**, 1700086.
31 U. De Silva, J. Masud, N. Zhang, Y. Hong, W. P. R. Liyanage, M. Asle Zaeem and M. Nath, *J. Mater. Chem. A*, 2018, **6**, 7608-7622.
32 J. Masud, P.-C. Ioannou, N. Levesanos, P. Kyritsis and M. Nath, *ChemSusChem*, 2016, **9**, 3128-3132.
33 J. Masud, W. P. R. Liyanage, X. Cao, A. Saxena and M. Nath, *ACS Appl. Energy Mater.*, 2018, **1**, 4075-4083.
34 Y. Wang, S. Liu, Y. Lai, Y. Zhu, R. Guo, Y. Xia, W. Huang and Z. Li, *Sens. Actuators, B*, 2018, **262**, 801-809.
35 W. Zhu, J. Wang, W. Zhang, N. Hu, J. Wang, L. Huang, R. Wang, Y. Suo and J. Wang, *J. Mater. Chem. B*, 2018, **6**, 718-724.
36 M. B. Gawande, A. Goswami, F.-X. Felpin, T. Asefa, X. Huang, R. Silva, X. Zou, R. Zboril and R. S. Varma, *Chem. Rev.*, 2016, **116**, 3722-3811.
37 X. Liu, X. Duan, P. Peng and W. Zheng, *Nanoscale*, 2011, **3**, 5090-5095.
38 K. G. Schick, V. G. Magearu and C. O. Huber, *Clin. Chem.*, 1978, **24**, 448-450.
39 X. Cao, E. Johnson and M. Nath, *ACS Sustainable Chem. Eng.*, 2019, **7**, 9588-9600.
40 X. Cao, Y. Hong, N. Zhang, Q. Chen, J. Masud, M. A. Zaeem and M. Nath, *ACS Catal.*, 2018, **8**, 8273-8289.
41 X. Liu, W. Yang, L. Chen and J. Jia, *Electrochim. Acta*, 2017, **235**, 519-526.
42 L. Zhang, C. Ye, X. Li, Y. Ding, H. Liang, G. Zhao and Y. Wang, *Nano-Micro Letters*, 2017, **10**, 28.
43 X. Zhang, J. Luo, P. Tang, J. R. Morante, J. Arbiol, C. Xu, Q. Li and J. Fransaer, *Sens. Actuators, B*, 2018, **254**, 272-281.
44 C. Zhao, X. Wu, X. Zhang, P. Li and X. Qian, *J. Electroanal. Chem.*, 2017, **785**, 172-179.
45 F. Huang, Y. Zhong, J. Chen, S. Li, Y. Li, F. Wang and S. Feng, *Anal. Methods*, 2013, **5**, 3050-3055.
46 X. Luo, M. Huang, L. Bie, D. He, Y. Zhang and P. Jiang, *RSC Adv.*, 2017, **7**, 23093-23101.
47 C. Lee, S. H. Lee, M. Cho and Y. Lee, *Microchim. Acta*, 2016, **183**, 3285-3292.
48 K. Ghanbari and Z. Babaei, *Anal. Biochem.*, 2016, **498**, 37-46.
49 R. Ahmad, N. Tripathy, M.-S. Ahn, K. S. Bhat, T. Mahmoudi, Y. Wang, J.-Y. Yoo, D.-W. Kwon, H.-Y. Yang and Y.-B. Hahn, *Sci. Rep.*, 2017, **7**, 5715.